

Galectin-9 trafficking regulates apical-basal polarity in Madin–Darby canine kidney epithelial cells

Rashmi Mishra^a, Michal Grzybek^a, Toshiro Niki^b, Mitsuomi Hirashima^c, and Kai Simons^{a,1}

^aMax-Planck Institute of Molecular Cell Biology and Genetics, 01307 Dresden, Germany; ^bGalPharma Co., Ltd., Kagawa 761-0793, Japan; and ^cDepartment of Immunology and Immunopathology, Kagawa University, Kagawa 761-0793, Japan

Contributed by Kai Simons, August 25, 2010 (sent for review July 5, 2010)

Galectins are unconventionally secreted lectins that participate in the formation of glycoprotein lattices that perform a variety of cell surface functions. Galectins also bind glycosphingolipid headgroups with as yet unclear implications for cellular physiology. We report a specific interaction between galectin-9 and the Forssman glycosphingolipid (FGL) that is important for polarizing Madin–Darby canine kidney epithelial cells. Galectin-9 knockdown leads to a severe loss of epithelial polarity that can be rescued by addition of the recombinant protein. The FGL glycan is identified as the surface receptor that cycles galectin-9 to the Golgi apparatus from which the protein is recycled back to the apical surface. Together our results suggest a model wherein such glycosphingolipid–galectin couples form a circuit between the Golgi apparatus and the cell surface that in an epithelial context facilitates the apical sorting of proteins and lipids.

cellulogenesis | epithelial polarity | Forssman glycosphingolipid | protein–lipid interactions | raft clustering

Galectins constitute a family of β -galactoside-binding lectins that are synthesized in the cytoplasm and then secreted via an unconventional pathway, possibly by direct translocation across the plasma membrane or through the membrane of the trans-Golgi network (TGN) (1, 2). These proteins are conserved in most animal taxa, fungi, and plants, suggesting an important physiological role. However, a coherent picture is still lacking (3). Interestingly, galectin expression is regulated both temporally and spatially during tissue morphogenesis, particularly in polarized epithelia (4). In cellular epithelial models, two galectins, galectin-3 and -4, have been assigned functions in apical membrane sorting (5, 6). In intestinal HT-29 cells, galectin-4 was reported to associate with sulfatides to form sorting platforms for the delivery of raft proteins to the apical surface. Galectin-3, on the other hand, was proposed to assist in the apical delivery of nonraft proteins in polarized Madin–Darby canine kidney (MDCK) cells. Until now, the role that galectins play in the transport machinery has not been well understood.

In this study, we sought to define the molecular steps by which a galectin could interface with internal membrane trafficking processes. We chose galectin-9 (Gal-9) of the tandem-repeat galectin class bearing two linked carbohydrate recognition domains (CDR) (4, 7) for these studies. Although Gal-9 has been reported to modulate cell-surface adhesion in MDCK cells, it is secreted preferentially to the apical surface, suggesting a role for this protein apically (8). Interestingly, Gal-9 has high binding affinity to N-glycans and repeated oligolactosamines, resulting in a distinct preference for the Forssman pentasaccharide in vitro (9). The Forssman antigen is an apically residing glycolipid (10), representing the major glycosphingolipid (GSL) fraction in MDCK cells (11), and is required for epithelial polarization (12). With the stage set for a lipid-based connection to Gal-9 membrane trafficking, we could address the role that galectins play in epithelial cell morphology and polarization.

Results

Gal-9 Depletion Causes a Loss of Epithelial Polarity in MDCK Cells. Gal-9 knockdown MDCK cells (Gal-9 shRNA) were generated with a retrovirus-mediated shRNA system. A highly sensitive, electrochemiluminescence-based protein quantitation technique,

the Meso Scale Discovery (MSD) assay, revealed $86 \pm 7\%$ Gal-9 protein depletion 7 d posttransduction (Fig. 1A and *SI Materials and Methods*). Specificity of the shRNA construct was tested by a specific loss of EGFP signal from the stable MDCK cell lines expressing canine Gal-9–EGFP, whereas MDCK cells expressing shRNA-resistant human Gal-9–EGFP showed no such effect (Fig. 1B and C). Next, MDCK cells filter-grown for 5 d were immunostained for the tight-junction (TJ) protein zonula occludens 1 (ZO-1) and acetylated tubulin (a ciliary marker) (Fig. 1D). Mock-infected cells showed a mature cilium or at least the presence of a basal body from which the cilium grows. Gal-9 shRNA cells had only occasional rudimentary basal body staining (white arrowheads in Fig. 1D, *Right*), with no cilia. ZO-1 staining in Gal-9 shRNA cells showed enlarged, fusiform and mesenchymal-like morphology (Fig. 1D). The Gal-9–shRNA monolayer was less even, and the cells were flattened by a reduction in cell height (Fig. 1D, ZO-1, *x-z* view).

Striking differences in the localization of the endogenous apical and basolateral markers were observed between mock-infected and shRNA cells seeded at the same density on filters (Fig. 2A–H). In Gal-9–shRNA cells, the basolateral marker, E-cadherin, was observed on the free surface along with a dramatic intracellular accumulation (Fig. 2D, arrowhead). Also a mislocalization of an apical marker, carcinoma embryonic antigen (CEA), to the lateral surface was observed (Fig. 2H *x-z* view). These observations suggest that upon the treatment with Gal-9 shRNA, the distinct apical and basolateral compartments of the MDCK epithelial cells were reduced to free and adherent surfaces, respectively.

Gal-9 Deficiency Causes Delays in Apical Cargo Transport That Can Be Rescued with Recombinant Gal-9 Protein. We wanted to know whether the loss of the polarity axis in Gal-9 shRNA cells was caused by abnormalities in cargo transport from the major sorting station, the TGN. To study this possibility, we performed cell-surface arrival assays with apical raft-associated cargo, HA-M2-GFP (based on hemagglutinin fused to the cytoplasmic tail of influenza virus M2), and basolateral cargo, vesicular stomatitis virus glycoprotein VSVG-SP-GFP (SP, long spacer arm between VSVG and GFP) (13, 14) (*SI Materials and Methods*). The MSD assay revealed a fourfold decrease in surface delivery of HA-M2-GFP with a concomitant sixfold increase in plasma membrane accumulation of VSVG-SP-GFP in the Gal-9 shRNA cells vs. mock-infected cells (Fig. 3A and B). We tried to rescue the HA transport delays in the Gal-9 shRNA cells with an optimized dose of recombinant Gal-9 protein supplied from the apical side of the filter support used to culture these cells (*Materials and Methods* and Fig. S1). After 5 d of Gal-9 rescue regimen, we found that

Author contributions: R.M. and K.S. designed research; R.M. and M.G. performed research; T.N. and M.H. contributed new reagents/analytic tools; R.M., M.G., and K.S. analyzed data; and R.M. and K.S. wrote the paper.

The authors declare no conflict of interest.

Freely available online through the PNAS open access option.

¹To whom correspondence should be addressed: E-mail: simons@mpi-cbg.de.

This article contains supporting information online at www.pnas.org/lookup/suppl/doi:10.1073/pnas.1012424107/-DCSupplemental.

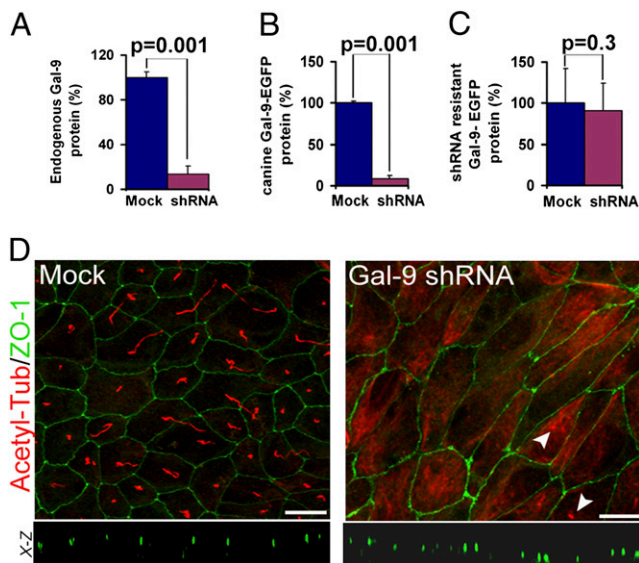


Fig. 1. Gal-9 depletion causes morphological and ciliogenesis defects. (A–C) A highly sensitive, electrochemiluminescence-based MSD technique was used to quantitate Gal-9 protein levels in retroviral shRNA-mediated knockdown cells. shRNA-susceptible canine and shRNA-resistant human Gal-9–EGFP constructs were stably expressed in MDCK cell lines to test the specificity of shRNA-mediated down-regulation. Samples were normalized to amounts of GAPDH. A one-tail, unpaired *t* test was used to generate *P* values. Error bars indicate SD. The data represent two mock-infected and shRNA cell pairs from three independent experimental groups. (D) Acetylated tubulin stains ciliary axoneme and basal body; ZO-1 reveals TJ areas. shRNA cells are enlarged, fusiform, and flat and show complete lack of cilium with occasional staining of the basal body (white arrowheads). (Scale bars: 10 μm .) The *x–z* view reveals TJs at varying heights.

the arrival of HA on the cell surface of Gal-9 shRNA cells treated with Gal-9 was comparable to that in untreated mock-infected counterparts. The functional recovery of the Gal-9–treated shRNA cells was substantiated further by a complete recovery of trans-epithelial resistance (TER), an index for the TJ integrity of an epithelial monolayer (Fig. 3D). TER measurements reflect that the TJs in the Gal-9 shRNA cells were not intact even though ZO-1 staining, a marker of TJ, could be observed (Fig. 1D). We found that Gal-9–treated shRNA cells had normal number of cilia when compared with mock-infected cells. Interestingly, a twofold increase in ciliary length was observed in the Gal-9–treated shRNA cells (Fig. 4A–C). However, could Gal-9 rescue the imbalances in the apical and basolateral markers observed in this study? To answer this question, we measured the total cell-surface expression of CEA and E-cadherin in mock-infected, Gal-9 shRNA, and Gal-9–treated shRNA cells. We found significant normalization of the steady-state protein levels of both apical and basolateral markers in the Gal-9–treated shRNA cells (Fig. 4D), and their normal localization was also restored (Fig. 4E). In contrast, addition of Gal-9 from the basal side of the Transwell filter failed to cause any significant recovery in polarity as assessed by TER measurements (Fig. S2).

Apically Enriched Forssman Glycosphingolipid Is a Receptor for Gal-9 in MDCK Cells. When added from the apical side of the filter support, exogenous Gal-9 rescued the polarity defects in Gal-9 shRNA cells. We also know that endogenous Gal-9 is apically secreted. These findings led us to investigate the cell-surface receptors for Gal-9 on the apical membrane. We know from a recent report that Gal-9 has a strong binding affinity for the Forssman pentasaccharide (9, 15). Interestingly, this glycan moiety is presented on a lipid in MDCK cells known as the Forssman glycosphingolipid (FGL). FGL is apically enriched and also is enriched in the raft-associated HA cargo fraction in MDCK cells (16, 17). We wanted

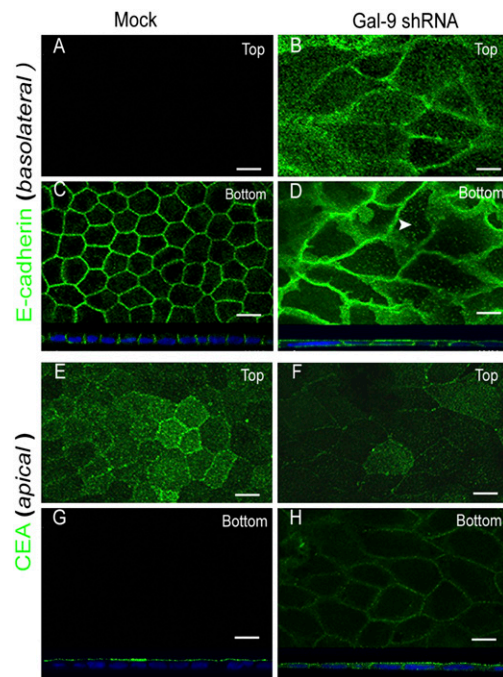


Fig. 2. Gal-9 depletion causes mislocalization of protein markers for apical and basolateral polarity. (A, C, E, and G) Mock-infected MDCK cells that were filter-grown for 5 d show E-cadherin localized to the basolateral membrane and CEA localized to the apical membrane. *Top*, merge of the three 0.5- μm slices farthest from the filter support used to grow the cells. *Bottom*, merge of three 0.5- μm slices near the filter support (attached surface). (B, D, F, and H) Gal-9 shRNA cells show E-cadherin and CEA expression in all planes, *x–z* views below C–D and G–H respectively. E-cadherin also showed an intracellular punctate staining (white arrowhead in D); (Scale bars: 10 μm .)

to know to what extent the FGL glycan epitope is required for Gal-9 binding to the apical membrane. We first confirmed Gal-9 binding to the FGL in an *in vitro* system (*SI Materials and Methods* and Fig. S3). To study the availability of this epitope on MDCK cells, we tried to mask the FGL glycan with different concentrations of an anti-FGL antibody, 12B12, characterized for its specificity for the Forssman antigen (12). We further confirmed the blocking activity of the 12B12 antibody through an *in vitro* competition assay (Fig. S3B). The binding of Gal-9 on MDCK cells was visualized and quantified in the presence and absence of the anti-FGL antibody. Rat IgG was included in the assay to negate any nonspecific antibody effects. Notably, Gal-9 binding to FGL glycan was found to decrease with a pH drop (Fig. S4). We therefore used this stripping step in the MSD assay to quantify the membrane-bound Gal-9. This information enabled us to strip membrane-bound biotin–Gal-9 and compare them with the unbound fractions in each experimental condition. The results showed a dramatic decrease in biotin–Gal-9 signals in conditions where higher concentrations of anti-FGL antibody were used (Fig. 5A and B). This result led us to conclude that the FGL glycan moiety is a major available target for Gal-9 on the apical surface of the MDCK cells. Although we cannot exclude the possibility that the 12B12 antibody also detects unknown Forssman-reactive glycoprotein, this FGL glycan moiety must play a significant role in the rescue of MDCK cell polarity by Gal-9. However, we confirmed the reproducibility of the above results on MDCK cells that were depleted of glycosphingolipids via inhibition of glucosylceramide synthase enzyme (Fig. S5). We further showed that Gal-9 shRNA mimics the effects reported for 12B12-mediated FGL inhibition with a similar loss in TER (Fig. S6) (12). FGL levels were reduced in Gal shRNA-treated MDCK cells, producing effects similar to those obtained via the 12B12 antibody blocking (Fig. S7). Further,

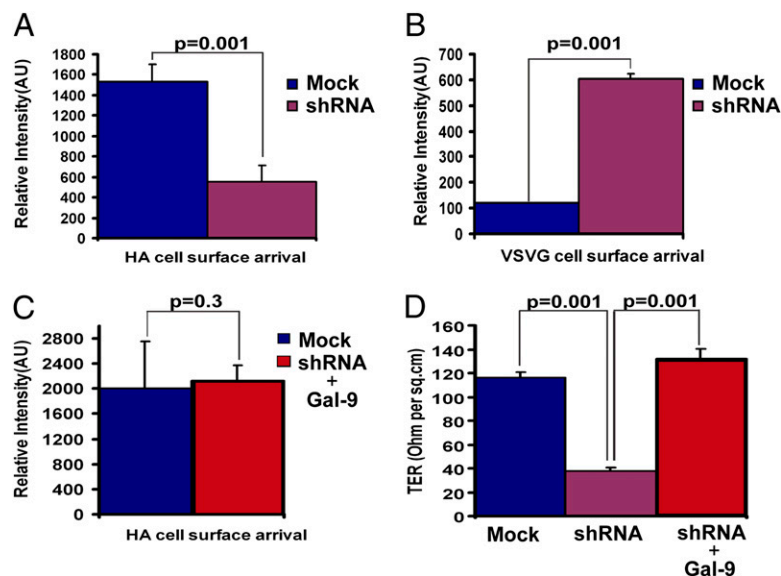


Fig. 3. Gal-9 depletion causes transport defects that are rescued with recombinant Gal-9 protein. Adenoviruses expressing the apical cargo protein HA-M2-GFP or basolateral cargo protein VSVG-SP-GFP were harvested for total cell-surface MSD-based transport assays. (A and B) HA surface signal was fourfold lower, and VSV-G surface signal was sixfold higher, after 45 min of cargo release from TGN as compared with the mock-infected cells. (C) shRNA cells were treated with 0.15 μ M recombinant Gal-9 for 5 d. The HA transport assay showed surface delivery comparable to mock-infected conditions. Samples in A–C are normalized to levels of GFP in lysates used to indicate transfection efficiency. (D) Gal-9-treated shRNA cells showed a recovery of TER comparable to levels in mock-infected cells. The data represent three independent experiments conducted in duplicate. *P* values were generated from a one-tailed, unpaired *t* test. Error bars indicate SD.

both binding/internalization and TER were significantly reduced in Gal-9 shRNA-infected cells that were treated with Gal-9 protein in the presence of 12B12 antibody (Fig. S8). These results confirm an essential role of FGL in Gal-9 internalization.

Gal-9 Is Internalized and Recycled Back to the Apical Membrane. Gal-9 rescues polarity, and it binds to FGL. How does FGL affect the

Gal-9 rescue function? Does it mediate Gal-9 internalization into the biosynthetic pathway to become an active component of the cargo-sorting machinery? This possibility was tested by binding biotin-Gal-9 to the apical surface of MDCK cells. After a brief pulse of endocytosis, a pH drop on ice was performed to remove uninternalized Gal-9. The cells were then incubated at 37 $^{\circ}$ C for various time intervals, fixed, immunostained with various cellular markers, and imaged to reveal the route of internalization of Gal-9. After internalization, biotin-Gal-9 was observed mainly in early

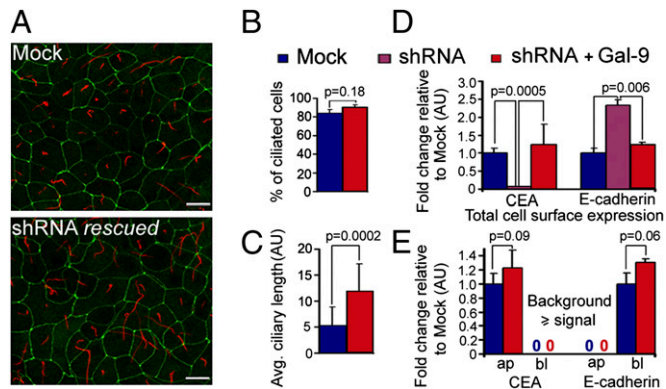


Fig. 4. Recombinant Gal-9 rescues ciliogenesis and steady-state expression of apical and basolateral marker proteins. (A) Filter-grown mock-infected and Gal-9-treated shRNA cells were immunostained with anti-acetylated tubulin to visualize the cilium. (Scale bar: 10 μ m.) (B and C) The number of cells positive for either a ciliary base or cilia in Gal-9-treated shRNA cells is comparable to the number in mock-infected cells, but the Gal-9-treated shRNA cells show a twofold increase in ciliary length. (D) Mock-, shRNA-, and Gal-9-treated shRNA cells were grown on a filter for 5 d, biotinylated from both sides of the filter, and subjected to MSD-based assay. (E) Mock- and Gal-9-treated shRNA cells were biotinylated from either the apical or the basolateral side and subjected to MSD assay to generate a steady-state profile of relative amounts of CEA and E-cadherin. Samples were normalized to amounts of GAPDH detected in cell lysates. The data represent the results of three independent experimental sets conducted in duplicate. ap, apical membrane; AU, arbitrary unit. bl, basolateral membrane. *P* values are generated from a one-tailed, unpaired *t* test. Error bars indicate SD.

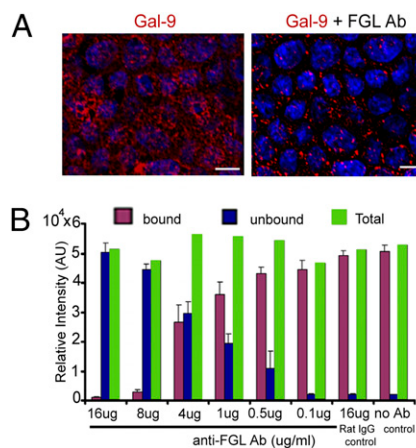


Fig. 5. FGL is a receptor for Gal-9 on the apical surface of MDCK cells. (A) Fully polarized MDCK epithelial cells were incubated with varying concentrations of anti-FGL antibody (μ g/mL) on ice for 45 min. Biotinylated recombinant Gal-9 (0.01 μ M) was allowed to bind for 1 h on ice. Cells were fixed, immunostained with anti-biotin antibody without permeabilizing the cells, and were counterstained with DAPI. (Scale bars: 10 μ m.) (B) The unbound fraction was collected, and the bound fraction was stripped from the cellular membrane with a pH drop. Biotin-Gal-9 in each sample was quantitated by MSD assay. Rat IgG was used to negate any nonspecific antibody-mediated effects. Green bars indicate the sum of bound and unbound fractions. The data represent results from three independent experimental sets performed in duplicate. Error bars indicate SD.

modify cell adhesion, or stabilize different protein receptors on the plasma membrane (15). These diverse functions have been hypothesized to result from the formation of galectin–glycan lattices that regulate cell surface glycoprotein organization and signaling (18). Impaired epithelial polarization by Gal-9 knockdown cells may reflect these functions. However, there is evidence for another interpretation for the role of this galectin. Previous studies on epithelial cells have demonstrated that galectins are involved in facilitating apical trafficking (6). Similarly we found that sorting and delivery of surface cargo proteins were impaired in the Gal-9 shRNA cells. Transport of the apical raft protein HA to the cell surface was slowed down, whereas the basolateral VSV-G was delivered to the plasma membrane more rapidly. Thus, trafficking problems could be a component of impaired polarization. How could Gal-9, being secreted unconventionally, be involved in the trafficking machinery? We now demonstrate the steps by which Gal-9 gains access to luminal biosynthetic sorting sites. Exogenous Gal-9 was endocytosed from the apical membrane into early endosomes, routed to the Golgi complex, and from there recycled to apical surface. Furthermore, FGL antibody competition experiments identified FGL as an apical receptor for Gal-9, in keeping with the specificity of its CDR. FGL is a major lipid constituent in MDCK apical membranes (11, 16, 19) and therefore probably is bound to Gal-9 during its internalization into the cell. Alternatively, Gal-9 could gain access to the TGN directly from the cytosol.

We propose a functional circuit of Gal-9 and FGL cycling between the Golgi and the apical membrane. This notion is consistent with two previous findings with respect to the epithelial biology of FGL. First, this GSL has been implicated in the biogenesis of epithelial cell-surface polarity by antibody-blocking experiments (19). Second, inhibitors of sphingolipid synthesis impair post-Golgi sorting in MDCK cells (20). Therefore, a circuit of Gal-9–FGL cycling could reinforce the polarization process. The apical membrane is known to behave like a percolating raft domain at 25 °C (21) and is dependent on glycosphingolipids for generating the protective lining of the epithelium barrier function by forming a boundary covering the cell layer (22). The Gal-9–FGL circuit could both generate and maintain this glycosphingolipid-rich membrane barrier. Galectins usually are multivalent, and thus they can cluster surface ligands (7). Also Gal-9, which we used for our rescue and internalization studies, was found to form oligomers (23). Our working hypothesis is that FGL–Gal-9 interactions in the TGN help nucleate a raft-clustering process to sort the distribution of cargo components laterally in the membrane plane. This process could be akin to the phase separation induced by pentavalent cholera toxin crosslinking of monosialotetrahexosylganglioside in plasma membrane spheres (24), during which raft proteins are included into the raft phase and nonraft proteins are excluded. In what state Gal-9 enters the TGN is not known, but we would assume that the Gal-9–FGL interactions must have been dissociated, at least partially, because of low endosomal/TGN pH (25) and/or by the ionic conditions (26). The unoccupied CDR on Gal-9 then could be available to bind to new FGL molecules. This scheme would enable raft clustering and lateral sorting in the TGN to trigger domain-induced budding into an apical raft carrier (27, 28). Further experimental work is needed to tell whether this speculative scheme holds true. Interestingly, galectin-4 in epithelial HT-29 cells binds to sulfatide, and this lectin–glycosphingolipid couple also is involved in sorting and delivery of raft-protein cargo to the apical surface (6).

The defective ciliogenesis that we observed in the Gal-9 shRNA cells also could be explained by the impairment of the delivery of surface cargo. We previously examined the effects of depleting different apical transport proteins in MDCK cells and noticed that many cells had impaired ciliogenesis, no matter which protein was knocked down (29). Ciliogenesis is a late stage in epithelial polarization (30). Thus, interfering with the development of epithelial polarity might coincidentally disturb cilia formation, especially if the machinery for generating functional apical and basolateral surface domains is defective. The ciliary membrane forms a differentiated part of the apical membrane, and its biogenesis is integrated with proper cell-surface polarization (10, 29).

In conclusion, we demonstrated that control of post-Golgi membrane trafficking by secreted Gal-9 is facilitated through specific interaction with glycolipids. This galectin–glycolipid circuit appears crucial to maintain epithelial integrity, revealing an interesting mechanism by which cells regulate their polarity.

Materials and Methods

Internalization of Gal-9 and Rescue Experiments. MDCK cells were cultured on Transwell polyester membrane inserts for 5 d. Gal-9 was biotinylated according to manufacturer's instructions (Pierce). For cellular studies, 0.01 μ M of Gal-9 was added to 200 μ L of CO₂-free medium with 5% FCS and glutamine. Cells were incubated for 30 min at 0 °C and washed to eliminate residual biotin–Gal-9. Then the cells were held at 37 °C for 15 min to allow internalization of the labeled protein, followed by a low-pH wash (20 mM glycine, pH 2.5) at 0 °C. The cells then were incubated at 37 °C for different time intervals up to 2 h and processed either for confocal microscopy or for MSD quantitation of Gal-9 recycling to the apical surface.

Gal-9-EGFP Construct. BAC CH82-319J05 or CH82-498E16, harboring canine *LGALS9*, and BAC RP11-19P22, containing human *LGALS9*, were obtained from the BACPAC Resources Center. Recombineering and stable transfection of the modified BACs were performed as described in ref. 31. Briefly, both BAC-tagging cassettes, localization and purification sequence (LAP) and fluorescent localization and purification sequence at the N terminus (NFLAP), were PCR amplified using primers that carry 50 nucleotides of homology to the insertion site. Next, a plasmid carrying two recombinases as well as the purified tagging cassette was electroporated into the *Escherichia coli* strain containing the BAC vector. Precise incorporation of the tagging cassette was confirmed by PCR and sequencing. Next, the EGFP-tagged BAC was isolated from bacteria using the Nucleobond PC100 kit (Macherey-Nagel). MDCK type II cells were transfected using Effectene (Qiagen) and cultivated in selection medium containing 400 μ g/mL Geneticin (G418; Invitrogen). Finally, MDCK cells stably expressing the tagged protein were sorted and selected by FACS to obtain populations of cells expressing high, medium, and low levels of EGFP. Cells expressing medium levels of EGFP were used for subsequent experiments.

Further information on reagents and antibodies, cell culture, RNAi, alamarBlue cell viability assay, measurement of transepithelial resistance, immunofluorescence, confocal microscopy, transport assay, MSD assay, and other methods is given in *SI Materials and Methods*.

ACKNOWLEDGMENTS. We thank Daniel Lingwood for critical reading of the manuscript and for constant support and discussions, Ünal Coskun for advice and help with experiments, Patrick Keller for help with protein labeling and ECL assays, Martina Augsburg and Ina Poser for help in generating MDCK type II cell lines stably expressing BAC Gal-9–EGFP, and Rashi Tiwari for help in lipid extraction. This work was supported by the European Union's Six Framework Programme, by the Partnership for Reform in Science, by Mathematics Grant LSHB-CT2007-037740, by Federal Ministry of Education and Support BioChance Plus Grant 0313827DFG Schwerpunktprogramm1175, by the European Science Foundation Lipid–Protein Interactions in Membrane Organization, and by the German Research Council Transregio 83 (to K.S.).

- Nickel W, Rabouille C (2009) Mechanisms of regulated unconventional protein secretion. *Nat Rev Mol Cell Biol* 10:148–155.
- Rémillard-Labrosse G, Mihai C, Duron J, Guay G, Lippé R (2009) Protein kinase D-dependent trafficking of the large Herpes simplex virus type 1 capsids from the TGN to plasma membrane. *Traffic* 10:1074–1083.
- Cooper DN (2002) Galectinomics: Finding themes in complexity. *Biochim Biophys Acta* 1572:209–231.

- Hughes RC (2004) Galectins in kidney development. *Glycoconj J* 19:621–629.
- Delacour D, et al. (2007) Apical sorting by galectin-3-dependent glycoprotein clustering. *Traffic* 8:379–388.
- Delacour D, et al. (2005) Galectin-4 and sulfatides in apical membrane trafficking in enterocyte-like cells. *J Cell Biol* 169:491–501.
- Rabinovich GA, Toscano MA, Jackson SS, Vasta GR (2007) Functions of cell surface galectin-glycoprotein lattices. *Curr Opin Struct Biol* 17:513–520.

8. Friedrichs J, et al. (2007) Contributions of galectin-3 and -9 to epithelial cell adhesion analyzed by single cell force spectroscopy. *J Biol Chem* 282:29375–29383.
9. Nagae M, et al. (2008) Structural analysis of the human galectin-9 N-terminal carbohydrate recognition domain reveals unexpected properties that differ from the mouse orthologue. *J Mol Biol* 375:119–135.
10. Vieira OV, et al. (2006) FAPP2, cilium formation, and compartmentalization of the apical membrane in polarized Madin-Darby canine kidney (MDCK) cells. *Proc Natl Acad Sci USA* 103:18556–18561.
11. Hansson GC, Simons K, van Meer G (1986) Two strains of the Madin-Darby canine kidney (MDCK) cell line have distinct glycosphingolipid compositions. *EMBO J* 5: 483–489.
12. Zinkl GM, Zuk A, van der Bijl P, van Meer G, Matlin KS (1996) An antiglycolipid antibody inhibits Madin-Darby canine kidney cell adhesion to laminin and interferes with basolateral polarization and tight junction formation. *J Cell Biol* 133:695–708.
13. Schuck S, et al. (2007) Rab10 is involved in basolateral transport in polarized Madin-Darby canine kidney cells. *Traffic* 8:47–60.
14. Keller P, Toomre D, Díaz E, White J, Simons K (2001) Multicolour imaging of post-Golgi sorting and trafficking in live cells. *Nat Cell Biol* 3:140–149.
15. Garner OB, Baum LG (2008) Galectin-glycan lattices regulate cell-surface glycoprotein organization and signalling. *Biochem Soc Trans* 36:1472–1477.
16. van Genderen IL, van Meer G, Slot JW, Geuze HJ, Voorhout WF (1991) Subcellular localization of Forssman glycolipid in epithelial MDCK cells by immunoelectronmicroscopy after freeze-substitution. *J Cell Biol* 115:1009–1019.
17. Brown DA, Rose JK (1992) Sorting of GPI-anchored proteins to glycolipid-enriched membrane subdomains during transport to the apical cell surface. *Cell* 68:533–544.
18. Lajoie P, Goetz JG, Dennis JW, Nabi IR (2009) Lattices, rafts, and scaffolds: Domain regulation of receptor signaling at the plasma membrane. *J Cell Biol* 185:381–385.
19. Butor C, Stelzer EH, Sonnenberg A, Davoust J (1991) Apical and basal Forssman antigen in MDCK II cells: A morphological and quantitative study. *Eur J Cell Biol* 56: 269–285.
20. Mays RW, et al. (1995) Hierarchy of mechanisms involved in generating Na/K-ATPase polarity in MDCK epithelial cells. *J Cell Biol* 130:1105–1115.
21. Meder D, Moreno MJ, Verkade P, Vaz WL, Simons K (2006) Phase coexistence and connectivity in the apical membrane of polarized epithelial cells. *Proc Natl Acad Sci USA* 103:329–334.
22. Simons K, van Meer G (1988) Lipid sorting in epithelial cells. *Biochemistry* 27: 6197–6202.
23. Miyanishi N, et al. (2007) Carbohydrate-recognition domains of galectin-9 are involved in intermolecular interaction with galectin-9 itself and other members of the galectin family. *Glycobiology* 17:423–432.
24. Lingwood D, Ries J, Schwille P, Simons K (2008) Plasma membranes are poised for activation of raft phase coalescence at physiological temperature. *Proc Natl Acad Sci USA* 105:10005–10010.
25. Casey JR, Grinstein S, Orlowski J (2010) Sensors and regulators of intracellular pH. *Nat Rev Mol Cell Biol* 11:50–61.
26. Faucon JF, Dufourcq J, Couraud F, Rochat H (1979) Lipid-protein interactions. A comparative study of the binding of cardiotoxins and neurotoxins to phospholipid vesicles. *Biochim Biophys Acta* 554:332–339.
27. Schuck S, Simons K (2004) Polarized sorting in epithelial cells: Raft clustering and the biogenesis of the apical membrane. *J Cell Sci* 117:5955–5964.
28. Paladino S, et al. (2004) Protein oligomerization modulates raft partitioning and apical sorting of GPI-anchored proteins. *J Cell Biol* 167:699–709.
29. Torkko JM, Manninen A, Schuck S, Simons K (2008) Depletion of apical transport proteins perturbs epithelial cyst formation and ciliogenesis. *J Cell Sci* 121: 1193–1203.
30. Bacallao R, et al. (1989) The subcellular organization of Madin-Darby canine kidney cells during the formation of a polarized epithelium. *J Cell Biol* 109:2817–2832.
31. Poser I, et al. (2008) BAC TransgeneOmics: A high-throughput method for exploration of protein function in mammals. *Nat Methods* 5:409–415.